


# Involvement of FAK/P38 Signaling Pathways in Mediating the Enhanced Osteogenesis Induced by Nano-Graphene Oxide Modification on Titanium Implant Surface

This article was published in the following Dove Press journal:  
*International Journal of Nanomedicine*

Qingfan Li <sup>1,2</sup>  
Zuolin Wang<sup>1,2</sup>

<sup>1</sup>Shanghai Engineering Research Center of Tooth Restoration and Regeneration, Shanghai, People's Republic of China;

<sup>2</sup>Department of Oral Implant, School of Stomatology, Hospital of Stomatology, Tongji University, Shanghai, People's Republic of China

**Background:** Titanium implants are widely used in dental and orthopedic medicine. Nevertheless, there is limited osteoinductive capability of titanium leading to a poor or delayed osseointegration, which might cause the failure of the implant therapy. Therefore, appropriate modification on the titanium surface for promoting osseointegration of existing implants is still pursued.

**Purpose:** Graphene oxide (GO) is a promising candidate to perform implant surface biofunctionalization for modulating the interactions between implant surface and cells. So the objective of this study was to fabricate a bioactive GO-modified titanium implant surface with excellent osteoinductive potential and further investigate the underlying biological mechanisms.

**Materials and Methods:** The large particle sandblasting and acid etching (SLA, commonly used in clinical practice) surface as a control group was first developed and then the nano-GO was deposited on the SLA surface via an ultrasonic atomization spraying technique to create the SLA/GO group. Their effects on rat bone marrow mesenchymal stem cells (BMSCs) responsive behaviors were assessed in vitro, and the underlying biological mechanisms were further systematically investigated. Moreover, the osteogenesis performance in vivo was also evaluated.

**Results:** The results showed that GO coating was fabricated on the titanium substrates successfully, which endowed SLA surface with the improved hydrophilicity and protein adsorption capacity. Compared with the SLA surface, the GO-modified surface favored cell adhesion and spreading, and significantly improved cell proliferation and osteogenic differentiation of BMSCs in vitro. Furthermore, the FAK/P38 signaling pathways were proven to be involved in the enhanced osteogenic differentiation of BMSCs, accompanied by the upregulated expression of focal adhesion (vinculin) on the GO coated surface. The enhanced bone regeneration ability of GO-modified implants when inserted into rat femurs was also observed and confirmed that the GO coating induced accelerated osseointegration and osteogenesis in vivo.

**Conclusion:** GO modification on titanium implant surface has potential applications for achieving rapid bone-implant integration through the mediation of FAK/P38 signaling pathways.

**Keywords:** graphene oxide, SLA, titanium implant, osteogenic differentiation, osseointegration, cell signaling pathways

Correspondence: Zuolin Wang  
Shanghai Engineering Research Center of Tooth Restoration and Regeneration, Department of Oral Implant, School of Stomatology, Tongji University, 399 Yanchang Road, Shanghai 200072, People's Republic of China  
Tel +86-21-66313725  
Fax +86-21-66524025  
Email zuolin@tongji.edu.cn

## Introduction

Titanium-based implants are widely used as clinical bone inserts due to their excellent mechanical properties and good biocompatibility.<sup>1-4</sup> Nevertheless, commercial

titanium implants cannot fully meet clinical needs because of their limited osseointegration and osteoinductive properties, especially in cases of poor or inadequate bone conditions. Although implant surface modification at the micrometer scale through sandblasting and acid etching (SLA) has been confirmed to enhance the biological responses of cells *in vitro*,<sup>5</sup> it still takes 3–6 months to achieve good osseointegration to complete the repair in clinical practices. It is clear that molecular and cellular interactions between implanted devices and surrounding tissues are essential to bone-implant integration. Previous studies have also shown that the physical, chemical and biological characteristics of the material surface regulate the proliferation, adhesion, growth and differentiation of cells.<sup>6,7</sup> Considering this, appropriate modifications should be made on the existing titanium implant surface to guide the biological behavior of cells and thus to improve osseointegration and the performance of the implant. Thus far, various surface modification methods have been developed to improve the bioactivity of implants.<sup>8–10</sup> For instance, hydroxyapatite (HA) has components similar to bone tissue and is often used as an implant surface coating; however, although HA shows good biocompatibility *in vitro*, it cannot induce sufficient bone formation *in vivo*.<sup>11</sup> Magnesium, zinc, strontium and calcium can also be injected into the implant surface to optimize the surface properties, which is beneficial for promoting the adhesion, proliferation and osteogenic differentiation of rat bone mesenchymal stem cells (rBMSCs) and improving the osseointegration ability of the implant.<sup>12–15</sup> However, the equipment cost for ion implantation is high and carries the potential risk of toxicity. In addition, bioactive molecules such as growth factors (BMP-2, TGF- $\beta$ ), enzymes (ALP), proteins and polypeptides (collagen, osteopontin, RGD polypeptide) can be fixed on the surface of titanium to increase its biological activity.<sup>16</sup> However, disadvantages such as irritating side effects, high dosage requirements and associated high costs have limited their clinical applications.<sup>17</sup>

Graphene oxide (GO) is an oxygen-containing derivative of graphene, which is a new kind of two-dimensional carbon nanomaterial.<sup>18</sup> Due to the large number of oxygen-containing active functional groups on its surface, such as carboxyl and hydroxyl groups, it is easy to perform the biomaterial functionalized modification by GO, so GO has good application prospects in the biomedical field.<sup>19–21</sup> Kim et al<sup>22</sup> synthesized GO/calcium carbonate composites that showed good cellular biocompatibility with osteoblasts and promoted the osteogenic activity of materials *in vitro*. Moreover, a chitosan-GO scaffold

material has been synthesized by covalent linkage. The addition of GO not only reduced the degradation rate of chitosan but also enhanced the attachment and proliferation of MC3T3-E1 mouse preosteoblast cells.<sup>23</sup> More importantly, recent studies have suggested that GO can promote the adhesion, growth and osteogenic differentiation of stem cells. For instance, incorporating GO with calcium phosphate nanoparticles to synthesize nanocomposites, which had significant synergistic effects on accelerating the differentiation of human mesenchymal stem cells (hMSCs) into osteoblasts.<sup>24</sup> Lee et al<sup>25</sup> reported that the cellular proliferation and osteogenic differentiation of mesenchymal stem cells (MSCs) on GO substrates is higher than that on polydimethylsiloxane (PDMS) substrates. In addition, GO is also widely used in drug delivery<sup>26–28</sup> as well as antibacterial applications.<sup>29–31</sup> In summary, besides the combination of graphene oxide with other biomaterials, GO might have great potential as a surface modification material for dental or orthopedic titanium implants and may impart enhanced biological properties to the material surface. Although previous studies have explored cell responses to GO biomaterials, there has been no comprehensive evaluation of the cell responses *in vitro* and the osteogenesis effects *in vivo* of GO modification on SLA-treated titanium substrates. Moreover, little is known about the intracellular events that determine the effect of GO modification on bone-forming ability.

Given the abovementioned findings and uncertainties, we first constructed a surface structure on a titanium substrate by SLA as a control (denoted as the SLA surface), and then an ultrasonic atomization spraying technique, which has been previously reported as an excellent coating method for nanomaterials, was applied to coat the SLA surface with GO in order to develop a GO-modified material surface (denoted as the SLA/GO surface). Then, the characteristics of these two surfaces, including the surface morphology, elemental composition, wettability and protein adsorption capacity, were assessed. Next, we investigated the biological responses of bone marrow mesenchymal stem cells (BMSCs), such as cell adhesion, proliferation and osteogenic differentiation, induced by GO modification *in vitro* and the osseointegration performance *in vivo*. Moreover, the underlying biological mechanisms of osteogenic differentiation triggered by GO coating were systematically studied. The results suggest that GO modification on SLA-treated titanium surfaces exerts osteoinductive effects on BMSCs through

mediation of FAK and its downstream MAPK/P38 signaling pathway, which provides evidence for designing or fabricating ideal implants for dental or orthopedic medicine.

## Materials and Methods

### Preparation of the GO-Modified Titanium Substrates

Pure titanium substrates of grade IV with a size of  $10 \times 10 \times 1$  mm were sandblasted with large  $\text{Al}_2\text{O}_3$  grits under a pressure of 5 bar, and the perpendicular distance from the spray head to the substrate surface was 10 cm. Then, the titanium substrates were acid etched in a mixture of HCl and  $\text{H}_2\text{SO}_4$  in a  $60^\circ\text{C}$  water bath for 8 h to obtain SLA titanium surfaces according to the methods in a previous report<sup>32</sup> at the Shanghai Institute of Ceramics, Chinese Academy of Sciences (Shanghai, China). Then, the SLA-treated materials were immersed in a 3% solution of (3-aminopropyl)-triethoxysilane (APTES) for 1 h to introduce positive amine groups on the material surface.<sup>33</sup> Afterward, GO was deposited on the SLA titanium surfaces via the ultrasonic atomization spraying technique by a specific apparatus (Siansonic, China) at the School of Materials Science and Engineering, University of Shanghai for Science and Technology (Shanghai, China). The specific parameters were as follows: the GO dispersion was pumped to the nozzle at  $250 \mu\text{L}/\text{min}$ , the spraying distance (from the atomizer outlet to the material surface) was 10 cm, and the spraying time was 90 s. The concentration of GO in the solutions used in all of the coating experiments was fixed at 0.05% (w/v), according to the literature.<sup>34</sup> The resulting samples were cleaned with anhydrous ethanol and ultrapure water before use. Samples treated only with SLA were used as controls and are referred to as the SLA samples. The SLA-treated samples coated with GO are referred to as the SLA/GO samples. To further investigate the effect of GO modification on osteogenesis in vivo, microimplants (outside diameter 2.2 mm, length 3.5 mm, thread depth 0.35 mm and thread distance 0.7 mm) with SLA or SLA/GO surfaces (prepared with the same method described above) were fabricated in advance.

### Characterization of the GO-Modified Titanium Substrates

A field emission scanning electron microscope (FE-SEM, S-4800, Hitachi, Japan) with an accelerating voltage of 5.0 kV was used to investigate the surface topography and

elemental analysis. Raman spectra from 1000 to  $3000 \text{ cm}^{-1}$  were obtained using a Raman microscope system (Lab-RAM, Horiba Jobin Yvon, France) with an Ar-ion laser at 20 Mm and a wavelength at 532 nm. A contact angle instrument (DSA100, Kruss, Germany) was applied to evaluate the hydrophilic-hydrophobic properties of the various surfaces. The protein adsorption capacity of the material surfaces were determined as follows: after the materials were immersed in a 1 mg/mL bovine serum albumin (BSA, Biosharp, China) solution in a 24-well cell culture plate for 24 h, the unadhered proteins were washed with phosphate-buffered saline (PBS), the proteins adhered to the material surface were washed with 2% sodium dodecyl sulfate (SDS, Sigma, USA), and the protein concentration was determined with a BCA protein quantitation assay kit (Beyotime, China).

### Isolation and Culture of Rat BMSCs

The Sprague-Dawley (SD) rats used in this research were purchased from the Laboratory Animal Center, Tongji University (Shanghai, China). BMSCs were isolated from the bilateral femurs of 4-week-old SD rats as described earlier.<sup>35</sup> The rat femurs were separated, and bone marrow was flushed out using complete medium, which consisted of modified Minimum Essential Medium Eagle Alpha ( $\alpha$ -MEM, Gibco, USA) with 1% streptomycin and penicillin (HyClone, USA) and 10% fetal bovine serum (FBS, Excell, Australia). The flushed bone marrow was then placed in an incubator at  $37^\circ\text{C}$  with 5%  $\text{CO}_2$  to allow the cells (ie, primary BMSCs) to adhere. After 72 h, the unadhered cells and impurities were removed by washing the cells with PBS. The cell culture medium was changed every two days. When the cells reached approximately 80% confluence, cell passaging was performed. Passage 3–4 cells were seeded on the material surfaces for subsequent experiments.

### Cytocompatibility of the GO-Modified Titanium Substrates

Live/Dead Cell Double Staining Kits were used to evaluate the cytocompatibility of the GO-modified titanium substrates. Samples with different surfaces were placed in 24-well cell culture plates. The BMSCs were then inoculated onto the material surfaces at a density of  $2 \times 10^4$  cells per well and cultured for 48 h. After washing the cells with PBS 3 times, a working solution including Calcein-AM and propidium iodide (PI) was added into the cell culture plates, and the plates were incubated for 30 min with protection from

light according to the manufacturer's instructions (Yeasen, China). The cells were imaged using a fluorescence microscope with excitation/emission wavelengths of 490/515 nm for live cells and 535/617 nm for dead cells, respectively. The percentage of live cells was calculated using ImageJ software.

## Proliferation of BMSCs Cultured on the GO-Modified Titanium Substrates

A Cell Counting Kit-8 (CCK-8) assay was used to evaluate the effect of GO coating on cell proliferation at 1, 3, and 5 days after inoculation according to the instructions (Dojindo, Japan). At each specific time point, the material samples were transferred to new 24-well cell culture plates. Then, the CCK-8 solution was mixed with complete medium at a 1:10 ratio and added to the cell culture plate, and the cells were incubated at 37°C for 3 h. Finally, the absorbance at 450 nm was measured with a microplate reader (Tecan Infinite M200, Switzerland).

## Adhesion and Spreading of BMSCs Cultured on the GO-Modified Titanium Substrates

SEM was used to observe cell adhesion. After 24 h of cell culture, PBS solution was used to rinse the cells 3 times, and then the cells were fixed with 2.5% glutaraldehyde at 4°C overnight. The next day, the cells were dehydrated with an ethanol gradient. Tert-butanol (700 µL) was added to each well of the 24-well cell culture plate, and the plate was placed at -20°C for 30 min. Then, the cells were freeze-dried for 3 h. Cell adhesion was observed by SEM subsequently.

Cell F-actin cytoskeletal staining was applied to investigate cell morphology at an early stage. BMSCs were seeded onto the SLA/GO and SLA sample surfaces for 24 h. Then, the cells were fixed with 4% paraformaldehyde (PFA), permeabilized with 0.1% Triton X-100, and blocked with BSA solution. FITC-phalloidin (1:200, Sigma, USA) was used to label the cytoskeletons for 45 min. 4',6-Diamidino-2-phenylindole (DAPI, 1:1000, Sigma, USA) was used to label the cell nuclei for 15 min. The cells were then observed by confocal laser scanning microscopy (CLSM, Leica, Germany). ImageJ software was used to assess the single-cell area on each sample according to the methods in a previous study.<sup>36</sup>

## Osteogenic Differentiation of BMSCs Cultured on the GO-Modified Titanium Substrates

### Alkaline Phosphatase (ALP) Activity

After 4 and 7 days of culture of BMSCs on the SLA or SLA/GO surfaces, ALP activity analysis was conducted. Cells were rinsed with PBS 3 times and then permeabilized with 0.1% Triton X-100. Lysates were collected and centrifuged at 12,000 rpm at 4°C for 10 min. The total protein concentration was measured with a BCA protein quantitation assay kit. Finally, ALP activity was measured with a commercial ALP activity assay kit (Jiancheng, China) following the manufacturer's instructions.

### Extracellular Matrix (ECM) Mineralization

Alizarin red staining was applied to investigate the ECM mineralization of BMSCs cultured on the material surfaces. After 21 days of culture, cells were rinsed with PBS 3 times, fixed with 4% PFA solution for 30 min, and then stained with 40 mM alizarin red (Cyagen, USA). Ten percent cetylpyridinium chloride was added to dissolve the stain for the quantitative assay. Then, the absorbance at 562 nm was measured.

### Osteogenesis-Related Gene Expression

The expression of osteogenesis-related genes was investigated by reverse transcription-polymerase chain reaction (RT-PCR). BMSCs were cultured for 4 and 7 days, and cells on the material surfaces were lysed by TRIzol (Roche, Switzerland) for 30 min at 4°C. The lysates were collected in RNase-free EP tubes. RNA was extracted by isopropanol and reverse transcribed into cDNA using a Transcriptor First Strand cDNA Synthesis Kit (Takara, Japan). PCR was conducted with a FastStart Universal SYBR Green Master kit (Roche, Switzerland) using a thermal cycler (LightCycler<sup>®</sup> 96, Roche, Switzerland). The expression of target genes, including ALP, runt-related transcription factor 2 (RUNX2), osteopontin (OPN) and osteocalcin (OCN), was normalized to that of the housekeeping gene GAPDH. The primer sequences used in this study are listed in [Table 1](#).

## Focal Adhesion (Vinculin) Expression of BMSCs Cultured on the GO-Modified Titanium Substrates

The expression of vinculin was measured by RT-PCR. After 24 h of seeding, the BMSCs were washed with PBS for 3 times; then, the RNA was extracted and reverse

**Table 1** Primer Sequences Used in the RT-PCR Assay for BMSCs

Gene	Primer Sequences (F: Forward Primer; R: Reverse Primer)
RUNX2	F: 5'- CCATAACGGTCTTCACAAATCCT -3' R: 5'- TCTGTCTGTGCCTTCTGGTTC -3'
ALP	F: 5'- AACGTGGCCAAGAACATCATCA -3' R: 5'- TGTCCATCTCCAGCCGTGTC -3'
OCN	F: 5'- GGTGCAGACCTAGCAGACACCA -3' R: 5'- AGGTAGCGCCGGAGTCTATTCA -3'
OPN	F: 5'- GCGGTGAGTCTAAGGAGTCCC -3' R: 5'- TCAGATCCACGACGGACACA -3'
Vinculin	F: 5'- TGGACGGCAAAGCCATTCC -3' R: 5'- GCTGGTGGCATATCTCTTTCAG -3'
GAPDH	F: 5'- GGCACAGTCAAGGCTGAGAATG -3' R: 5'- ATGGTGGTGAAGACGCCAGTA -3'

transcribed to cDNA, and PCR was performed as described above. The expression of focal adhesion-related gene, namely vinculin in this study, was assessed and normalized to that of GAPDH. The primers sequences used for RT-PCR are shown in Table 1. In addition, Western blot was also used to investigate the vinculin expression of BMSCs cultured on the GO-modified titanium substrates in protein levels.

## Molecular Mechanism Investigation

Western blot analysis was used to detect the molecular mechanisms of the responsive behaviors of BMSCs cultured on the different material surfaces. After 48 h of culture, the protein expression of focal adhesion kinase (FAK), phospho-FAK (p-FAK), extracellular signal-related kinase 1/2 (ERK1/2), phospho-ERK1/2 (p-ERK1/2), P38 MAP kinases (P38), phospho-P38 (p-P38), Jun amino-terminal kinase (JNK), and phospho-JNK (p-JNK) were analyzed, and the expression level of  $\beta$ -actin was used as a reference. For Western blot analysis, the cells were first lysed by RIPA buffer (Beyotime, China). A BCA protein quantitation assay kit was used to determine the total protein content in the extracted lysates. The proteins were isolated by SDS-PAGE and transferred to PVDF membranes (Millipore, USA). The PVDF membranes were blocked with 5% skimmed milk for 1 h and then incubated with various primary antibodies (all from CST, USA) overnight. The next day, the membranes were incubated with HRP-conjugated secondary antibodies

(CST, USA). The membranes were then washed with TBST solution 3 times, and the bands were visualized with Pierce ECL Western Blotting Substrate (Thermo Fisher Scientific, USA). Finally, the protein bands were obtained, and the grayscale values were quantitatively analyzed.

Additional experiments were designed to examine whether mediation of FAK/P38 pathways was related to the enhanced osteogenic differentiation of BMSCs triggered by GO modification. The FAK signaling pathway inhibitor PF573228 (1  $\mu$ M, Sigma, USA) was added to the cell medium. At the same time, the P38 signaling pathway inhibitor SB203580 (10  $\mu$ M, CST, USA) was also added to the corresponding medium. The expressions of FAK and p-FAK, P38 and p-P38 were detected by Western blot analysis as described above. In addition, the effects of signaling pathway-specific inhibitors on the osteogenic differentiation of BMSCs were detected by the methods described former.

## Osteogenesis of the GO-Modified Titanium Implants in vivo

The animal experimental procedure was approved by the Animal Care and Use Committee of Tongji University (No. TJLAC-017-033), following the Guide for the Care and Use of Laboratory Animals published by the Chinese National Academy of Sciences. Eighteen six-week-old SD rats were anesthetized using 5% chloral hydrate (100 mg/kg) by intraperitoneal injection. After shaving the hair, an approximately 1.5 cm incision was made in the skin, and the soft tissue and the periosteum were elevated to expose the surface of the distal femur. A 2-mm diameter twist drill was used to make one hole. The drilling site was irrigated with saline. Then, titanium implants with SLA or SLA/GO surface modifications were randomly inserted into the holes. Each animal received two implants.

### Histological Analysis of Bone-Implant Contact (BIC)

After 2 and 4 weeks, the specimens were prepared for histomorphometric analysis. The specimens were embedded in polymethylmethacrylate after fixation and dehydration, and hard tissue sections were prepared with a diamond circular saw system (Exakt 300 CL, Germany). Then, a grinding system (Exakt 400 CS, Germany) was applied to grind and polish the sections to a thickness of approximately 50  $\mu$ m. The sections were stained with van Gieson (V-G) stain (Solarbio, China). The BIC percentage was analyzed by ImageJ software.

## Sequential Fluorescence Double Labeling for Analysis of Osteogenesis

Different colors of fluorescein can bind to newly formed bone tissue around implants to mark bone formation at different time points. Alizarin red (30 mg/kg, Sigma, USA) and calcein (20 mg/kg, Sigma, USA) were injected by intraperitoneal injection at 2 and 4 weeks after implantation, respectively, and then, the samples were removed and histologically sectioned at 6 weeks. Laser scanning confocal microscopy with excitation/emission at 543/617 nm for alizarin red (red) and 488/517 nm for calcein (green) was used to observe new bone formation around the implants, and the area of fluorescence staining was calculated by ImageJ software.

## Statistical Analysis

All quantitative measurements were repeated at least three times separately. The data are presented as the mean  $\pm$  standard deviation. SPSS 22.0 statistical software was used to perform

the *t*-test for statistical analysis. Values of  $p < 0.05$  were deemed to indicate statistical significance.

## Results and Discussion

### Characterization of the GO-Modified Titanium Substrates

The scheme used to fabricate the GO-modified titanium substrates is illustrated in Figure 1A. The surface properties of biomaterials have profound influences on their biological activities and functions and play important roles in regulating a variety of intracellular signals and cellular behaviors, such as adhesion, proliferation, differentiation and apoptosis.<sup>37–39</sup> Therefore, analysis of the surface characteristics of implants is a key step in research on the interactions between cells and biomaterials, which affect the osseointegration between implant and bone tissue. As shown in Figure 1B, after SLA, the surface of the titanium substrate presented an irregular rough surface with visible pits of

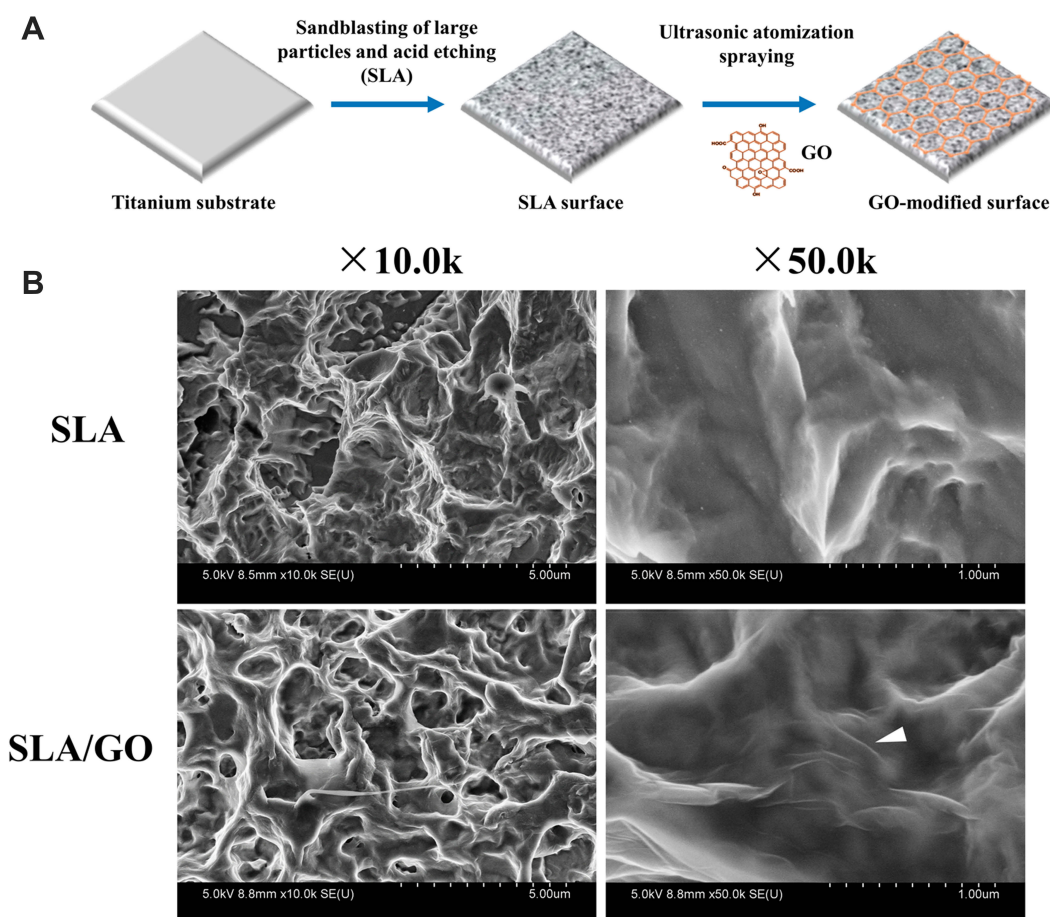


**Figure 1** (A) Scheme illustration for the fabrication process of the large particles sandblasting and acid etching (SLA) surface and the GO-modified (SLA/GO) surface. (B) The SEM images showing the surface topography of the SLA and SLA/GO samples. At 10.0 k magnification, rough irregular pitted surfaces were observed on the both groups, while the characteristic wrinkle-like structure of GO (as shown by the white arrow) was observed on the SLA/GO surfaces at 50.0 k magnification.

different sizes on the micro scale.<sup>40</sup> At low magnification, the GO-modified SLA surface also exhibited a pit-like structure. When magnified by 50,000 times, a characteristic wrinkle-like structure was overlaid on the surfaces of the samples, indicating that the substrates were successfully coated with GO, which results in a wrinkled structure.<sup>41</sup>

Energy Dispersive X-ray Spectroscopy (EDX) was used to determine the element types from SLA and SLA/GO surface. From Figure 2A, the spectrum on SLA/GO surface presented significant C and O peaks compared with the SLA surface, which was related to the successful coating of graphene oxide on the SLA-treated surface. Raman spectroscopy was also used to characterize the GO coating (Figure 2B). The Raman spectrum of the SLA surface was linear with no significant peaks. In contrast, the SLA surface modified by the GO coating exhibited characteristic peaks, including a D band at  $1350\text{ cm}^{-1}$  and a G band at  $1580\text{ cm}^{-1}$ , as shown; these results are consistent with those in previous reports.<sup>42,43</sup> These findings suggest that the GO retained its original structure after ultrasonic atomization spraying on the material surface. According to the literature, the D-band represents the defect level and crystallinity, and the G-band represents the  $\text{sp}^2$  graphitized structure.<sup>44</sup>

A contact angle test was used to evaluate the wettability of the material surface (Figure 3A). After GO coating, the

material surface possessed significantly smaller contact angles (SLA,  $96.28^\circ \pm 1.12$ , and SLA/GO,  $34.61^\circ \pm 1.98$ ), indicating that the hydrophilicity of the titanium surface was improved after GO modification. Compared with hydrophobic surfaces, hydrophilic surfaces are considered to be more conducive to the adsorption of ECM proteins, which can promote initial cell adhesion, proliferation, differentiation and bone tissue mineralization.<sup>45</sup> In addition, the protein adsorption capacity was detected using a BSA protein standard according to the methods in a previous report.<sup>35</sup> Figure 3B shows that the GO-modified material surface had a higher protein adsorption capacity than the SLA surface. The physical and chemical properties and wettability of a surface are the main factors affecting protein adsorption. Here, the GO-coated surface was more hydrophilic than the SLA surface, thus facilitating protein adsorption.<sup>46</sup> In addition, GO coatings can interact with proteins through electrostatic forces and hydrogen bonding, which also promote protein adsorption.<sup>47</sup>

## Cytocompatibility of the GO-Modified Titanium Substrates

The compatibility of biomaterials is the primary condition determining their applications. To test the biocompatibility of the GO-modified material in this study, BMSCs were

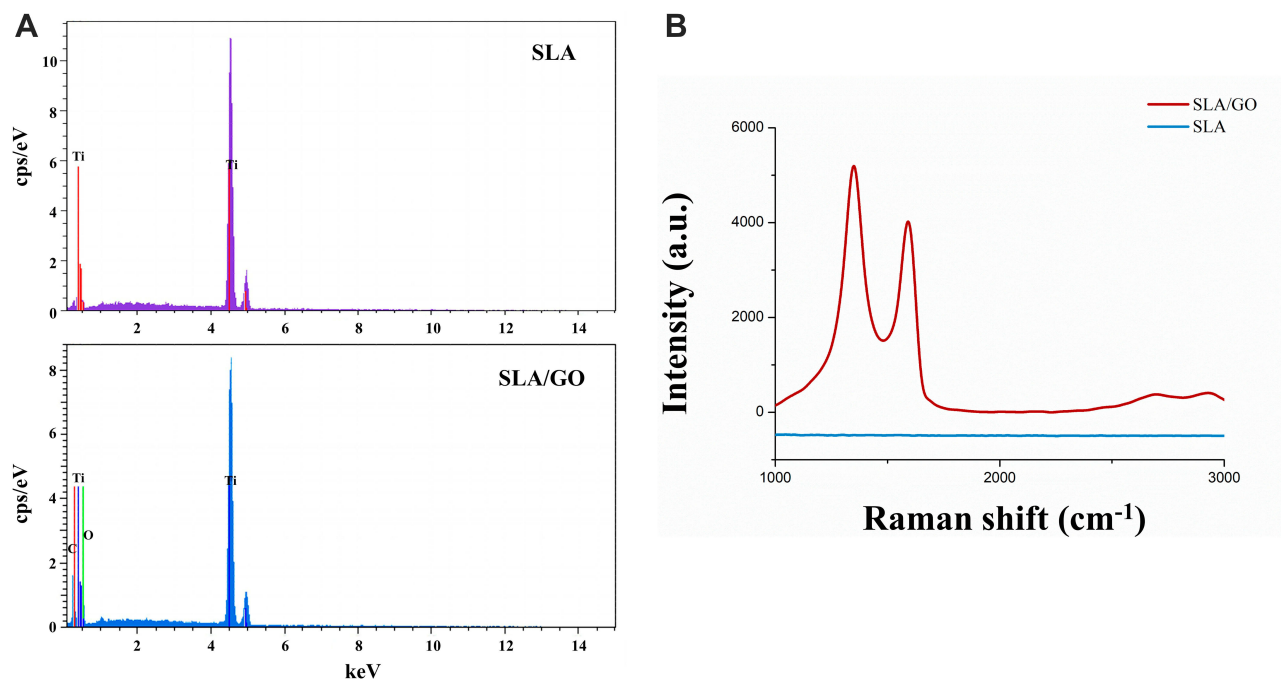


**Figure 2** Surface characterization of the SLA and SLA/GO samples. (A) Elemental analysis was evaluated by EDX, and significant carbon and oxygen peaks were presented on the SLA/GO surface compared with the SLA surface. (B) Raman spectra of the SLA and SLA/GO samples. Characteristic D band at  $\sim 1350\text{ cm}^{-1}$  and G band at  $\sim 1580\text{ cm}^{-1}$  were observed from SLA/GO surface, while a straight line from SLA surface.

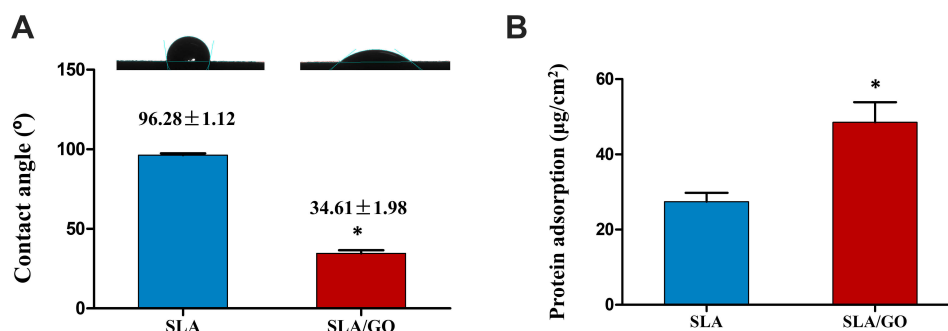


**Figure 3** Surface characterization of the SLA and SLA/GO samples. **(A)** Contact angle measurements showing the wettability of the samples. The SLA surface showed hydrophobic property and SLA/GO showed hydrophilic property. **(B)** Protein adsorption capacity of the SLA and SLA/GO samples was detected by immersing the material into the BSA protein solution and adhered protein was quantified. \* $p < 0.05$ .

seeded on the material surface, and the cells were stained with Calcein-AM and PI after 48 h of culture. In [Figure 4A](#), the cells with green fluorescence are live cells, while those with red fluorescence are dead cells. Analysis of the percent of live cells revealed no significant difference between the SLA and SLA/GO groups ([Figure 4B](#)), which indicates that the GO modification had no toxicity to cells and had good biocompatibility.<sup>48,49</sup>

### Proliferation of BMSCs Cultured on the GO-Modified Titanium Substrates

Cell proliferation was detected at 1, 3 and 5 days after inoculation by CCK-8 assay. According to [Figure 4C](#), there was no difference in cell proliferation between the SLA surface and the SLA/GO surface after 1 day of culture. However, at 3 days and 5 days after inoculation, the BMSCs cultured on the GO-modified material surface had higher proliferation than those cultured on the SLA surface ( $p < 0.05$ ). This indicates that GO modification is beneficial for cell proliferation.

### Adhesion and Spreading of BMSCs Cultured on the GO-Modified Titanium Substrates

To investigate the effect of GO coatings on cell adhesion, SEM was used to observe cell attachment on the material surface after 24 h of cell culture. As shown in [Figure 4C](#), the cells cultured on the SLA surface were relatively small in size and triangular in shape, while the BMSCs cultured on the SLA/GO surface were larger in size and polygonal in shape with numerous extended pseudopodia. This result suggests that the GO modification is conducive to cell adhesion on the material surface. Cell F-actin cytoskeletal staining was applied to investigate cell morphology and

spreading on the various surfaces. The nuclei were dyed blue with DAPI, and the cytoskeleton was dyed green with FITC-phalloidin. As shown in [Figure 4E](#), the BMSC extension area on the SLA/GO surface was larger than that on the SLA surface, and more cytoskeletal proteins were expressed on the SLA/GO surface than on the SLA surface. Quantitative analysis ([Figure 4F](#)) showed that the cells on the GO-modified surface were more than twice the size of those in the control group ( $p < 0.05$ ).

### Osteogenic Differentiation of BMSCs Cultured on the GO-Modified Titanium Substrates

ALP activity was analyzed to detect the early osteogenic differentiation of BMSCs on the various material surfaces. As shown in [Figure 5A](#), on both day 4 and day 7, the BMSCs cultured on the GO-modified material surface expressed more ALP than those cultured on the SLA material surface ( $p < 0.05$ ), which shows that GO modification obviously promotes early osteogenic differentiation of BMSCs.

Alizarin red staining was applied to investigate the ECM mineralization of BMSCs cultured on the material surfaces, as shown in [Figure 5B](#). After 21 days of culture, quantitative analysis of the alizarin red staining showed that BMSCs exhibited higher ECM mineralization on the SLA/GO surface than on the SLA surface ( $p < 0.05$ ). This result indicates that GO modification significantly enhances the original SLA-treated surface with regard to osteogenic differentiation of BMSCs.

The expression of osteogenesis-related genes was investigated by RT-PCR. BMSCs were cultured for 4 and 7 days, and the expression of characteristic osteogenesis-related genes, including ALP, RUNX2, OCN and OPN, was analyzed relative to that of the housekeeping gene

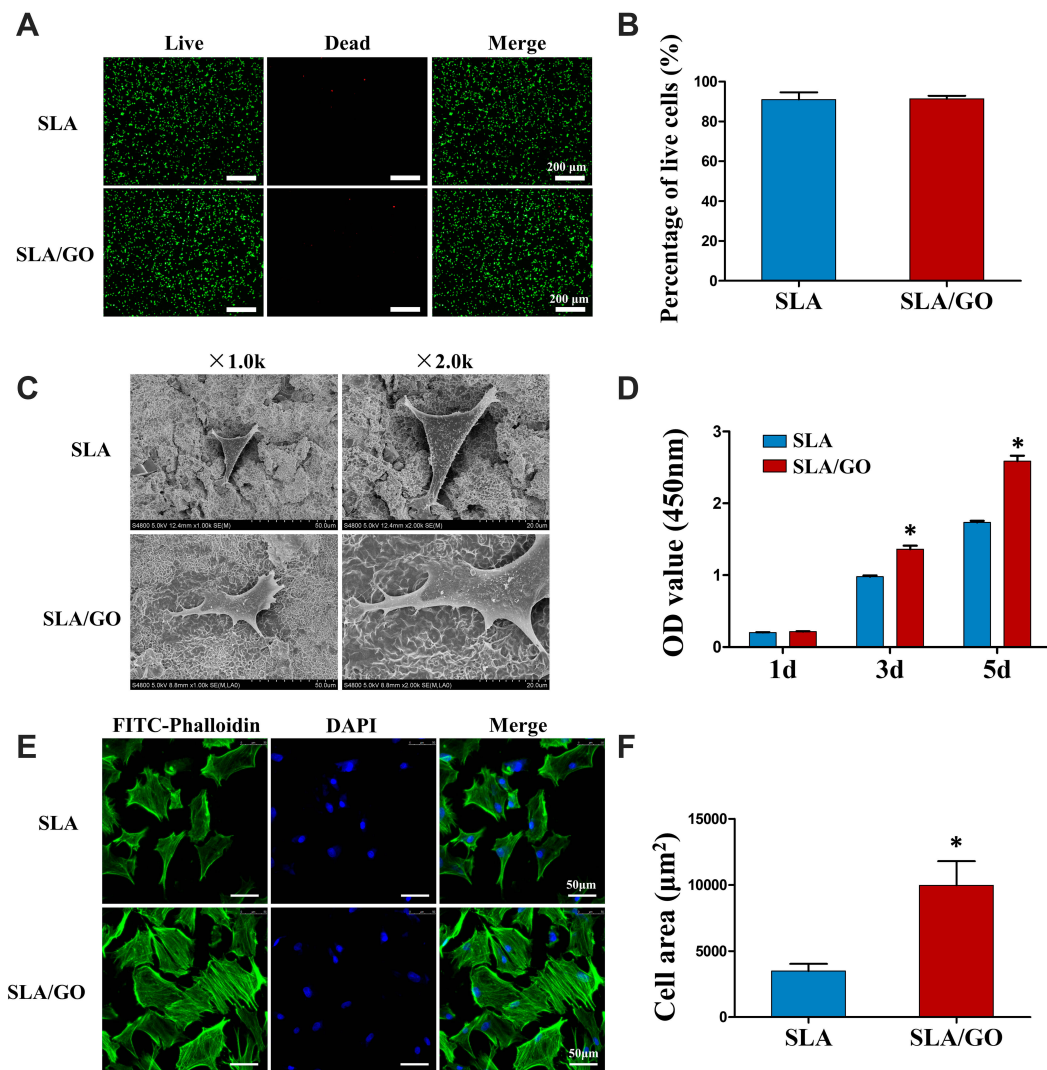


**Figure 4** (A) Fluorescent staining of live and dead BMSCs cultured on the SLA and SLA/GO samples surface (cells stained with red fluorescent were dead cells and green fluorescent were live cells) and (B) the percentage of live cells analyzed by ImageJ software. (C) Cell attachment of BMSCs cultured on the SLA and SLA/GO samples surface after 24 h of incubation. (D) Cell proliferation of BMSCs cultured on the SLA and SLA/GO samples surface at 1, 3 and 5 days. (E) Cell morphology of BMSCs cultured on the SLA and SLA/GO samples surface after 24 h of incubation and (F) average cell spreading area measured by ImageJ software. \* $p < 0.05$ .

GAPDH. ALP is an early marker of BMSC osteogenic differentiation, and RUNX2 is an osteoblast transcriptional activator that regulates the expression of osteoblastic genes and maintains early osteogenesis differentiation. OCN is a marker of late-stage bone formation and is closely related to osteoblast maturation and matrix mineralization and deposition. The noncollagenous protein OPN is also an important gene involved in bone matrix formation.<sup>50,51</sup> As shown in Figure 5C–F, the BMSCs cultured on the GO-modified surface more strongly expressed the relevant genes than those cultured on the SLA surface at both 4 days and 7 days ( $p < 0.05$ ), indicating that at both early and late stages, the osteogenic differentiation of BMSCs is upregulated by GO modification.

### Focal Adhesion (Vinculin) Expression of BMSCs Cultured on the GO-Modified Titanium Substrates

Focal adhesion (FA) are sites where cells are tightly bound to the ECM.<sup>52</sup> They can provide a structural link between the ECM and the cellular actin cytoskeleton.<sup>53</sup> More importantly, FA plays important role in regulating the signal transduction of cell adhesion, proliferation and differentiation. The experimental results in Figures 4 and 5 indicated that GO modification affected the adhesion, spreading, proliferation and osteogenic differentiation of BMSCs. We hypothesized that these changes in BMSCs might be associated with the expression of focal adhesion.

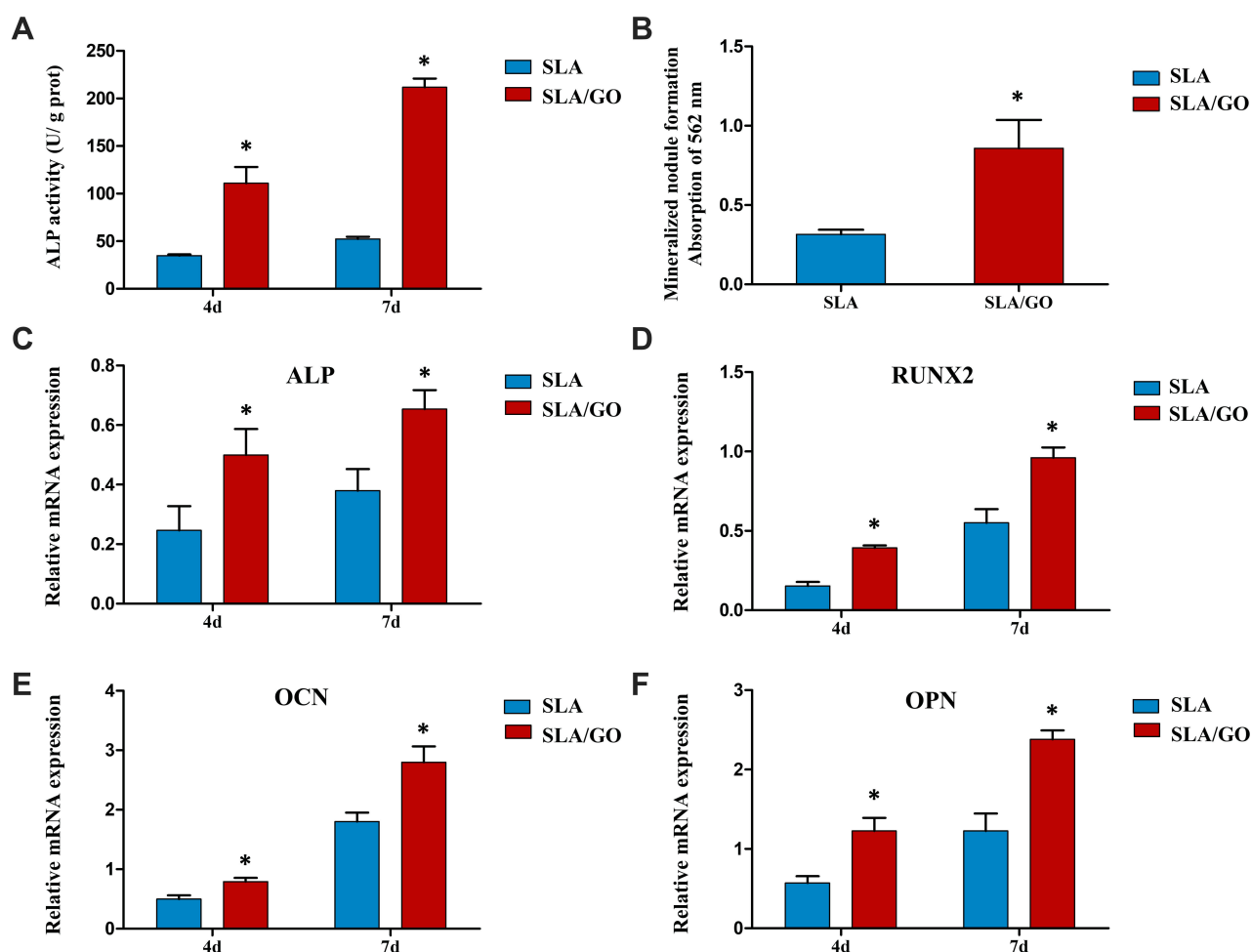


**Figure 5** Osteogenic differentiation of BMSCs cultured on the SLA and SLA/GO samples surface. (A) Quantitative analysis of the ALP activity of BMSCs for 4 and 7 days. (B) Quantitative analysis of the extracellular matrix mineralization of BMSCs for 21 days. The expressions of osteogenesis-related genes, including ALP (C), RUNX2 (D), OCN (E) and OPN (F), were detected by RT-PCR for 4 and 7 days. \* $p < 0.05$ .

In order to test the hypothesis above, the expression of vinculin, a high-content focal adhesion protein, was determined by RT-PCR and Western blot.<sup>54</sup> The results show that the expression of vinculin in BMSCs cultured on the

GO-modified surface was higher than that on the SLA surface (Figure 6). This suggests that GO modification alters FA, which likely exerts a profound impact on subsequent cell-biomaterial interactions.

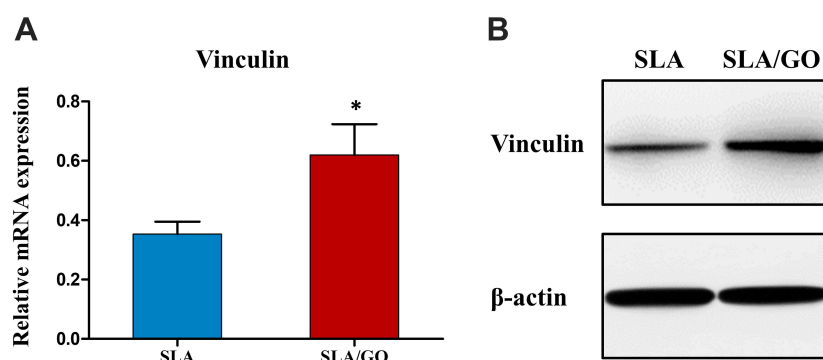


**Figure 6** Vinculin expressions of BMSCs cultured on the SLA and SLA/GO samples surface were detected by RT-PCR (A) and Western blot (B). \* $p < 0.05$ .

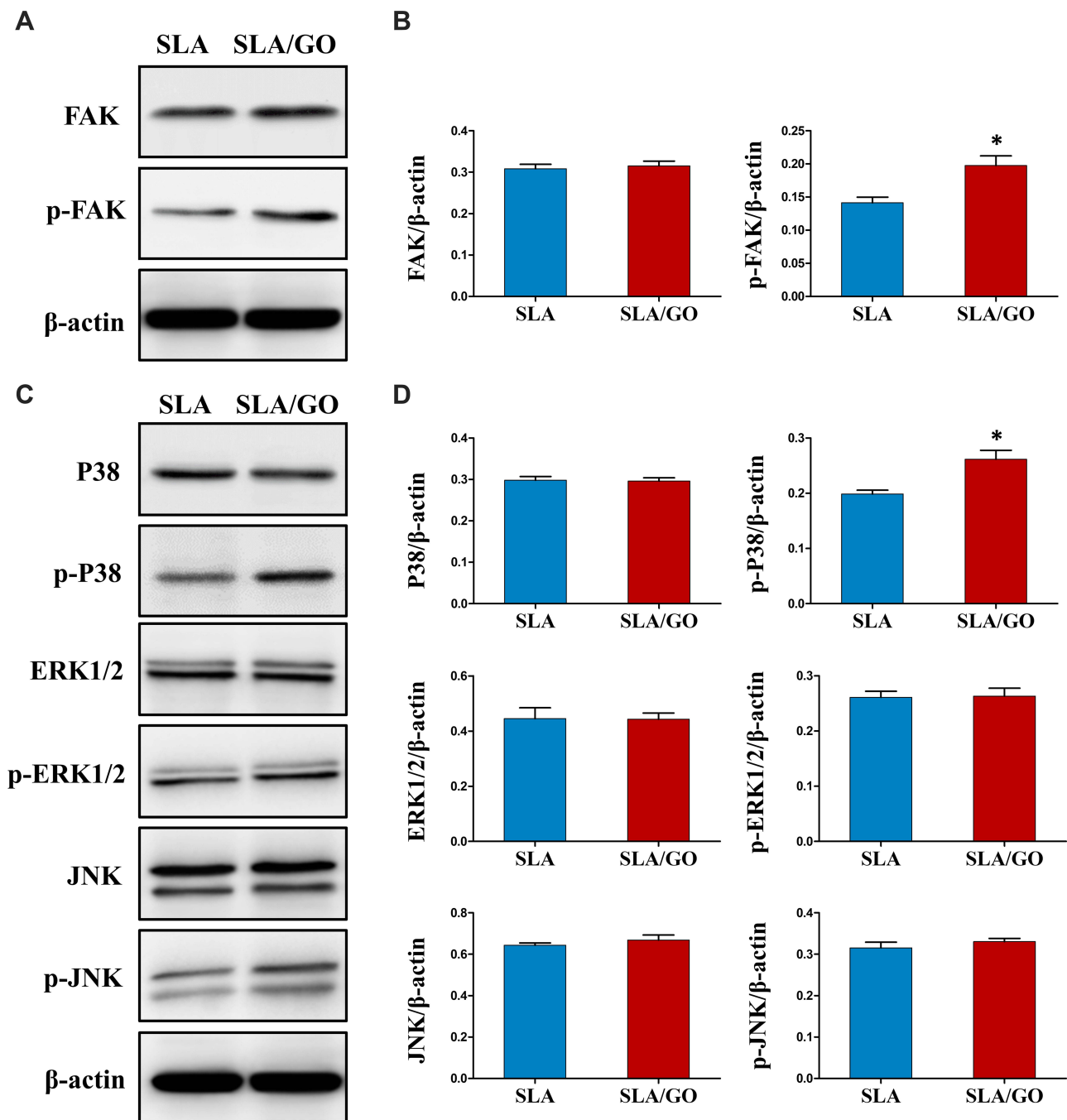


**Figure 7** (A) Western blot was used to assess the protein expressions of FAK, p-FAK of BMSCs cultured on the SLA and SLA/GO samples surface. (B) Quantitative analysis of the grayscale values for Western blot bands. (C) Protein expressions of MAPK signaling pathways, including P38, p-P38, ERK1/2, p-ERK1/2, JNK and p-JNK of BMSCs cultured on the SLA and SLA/GO samples surface, were detected by Western blot. (D) Quantitative analysis of the grayscale values for Western blot bands. \* $p < 0.05$ .

## FAK/MAPK Signaling Pathway Involvement in the Osteogenic Differentiation of BMSCs Cultured on the GO-Modified Titanium Substrates

It is well known that focal adhesion kinase (FAK) is an important member of the focal adhesion complex family,

influencing cell adhesion sites, the cytoskeleton, cell proliferation and migration.<sup>55,56</sup> Moreover, FAK is in a central position to participate in and modulate various downstream intracellular signaling pathways, such as mitogen-activated protein kinases (MAPK) signaling pathways, which are key mediators of cellular responses to a variety of extracellular stimuli. Therefore, in this experiment, we detected the

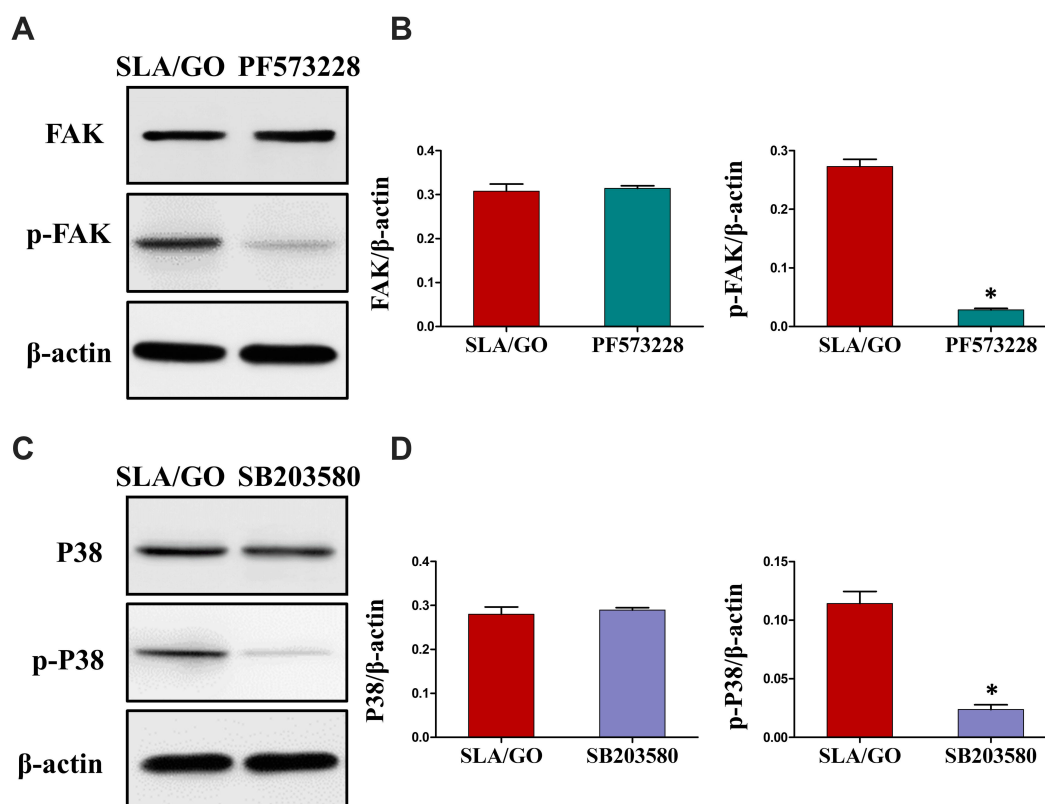


**Figure 8** (A) Western blot was used to detect the protein expressions of FAK, p-FAK of BMSCs cultured on the SLA and SLA/GO samples surface treated with or without specific inhibitors and (B) quantitative analysis of the grayscale values for Western blot bands. (C) Western blot analysis for the protein expressions of P38, p-P38 of BMSCs cultured on the SLA and SLA/GO samples surface treated with or without specific inhibitors and (D) quantitative analysis of the grayscale values for Western blot bands. PF573228 is the inhibitor of FAK and SB203580 is the inhibitor of P38. \* $p < 0.05$ .

expression of FAK and the expression of three main branches in the MAPK signaling pathway, namely, P38, ERK1/2, and JNK, by Western blot analysis of cells cultured on the SLA or SLA/GO material surface to reveal the connection between the FAK/MAPK signaling pathway and the enhanced osteogenic differentiation of BMSCs triggered by GO modification. The protein bands and the results of quantitative analysis of the grayscale values are presented in Figure 7. The results show that compared with those cultured on the SLA surface, the BMSCs cultured on the GO-coated surface expressed higher p-FAK (Figure 7A), which was confirmed by the results of quantitative analysis from Figure 7B ( $p < 0.05$ ). In addition, with regard to the 3 key MAPK signaling pathway proteins P38, ERK1/2, and JNK, p-P38 expression was noticeably higher in the BMSCs in the SLA/GO group than those in the SLA group (Figure 7C), as evidenced by the quantitative analysis of grayscale values ( $p < 0.05$ ), while p-ERK1/2 and p-JNK expression showed no significant differences between these two groups according to the Figure 7D ( $p > 0.05$ ). The above results show that GO modification can activate the

FAK and P38 signaling pathways and thus affect the biological functions of cells.

To verify the roles of the FAK and P38 signaling pathways in the osteogenic differentiation of BMSCs, the specific FAK and P38 inhibitors PF573228 and SB203580 were added to the BMSC medium, and then the expression of two key proteins, namely, FAK and P38, and the effect on the osteogenic differentiation of BMSCs were detected simultaneously. PF573228 has been confirmed to be a powerful and selective inhibitor of FAK.<sup>57</sup> In addition, PF573228 has been found to exert a mutual effect on the ATP-binding pocket of FAK, which can result in inhibition of the catalytic activity of the enzyme.<sup>58</sup> SB203580 is a widely used selective inhibitor of P38. SB203580 blocks the binding of P38 and ATP to inhibit the catalytic activity of P38.<sup>59</sup> The Western blot results in Figure 8A and B show that the protein expression level of p-FAK was significantly down-regulated by these specific inhibitors ( $p < 0.05$ ). Similarly, the expression level of p-P38 was inhibited by SB203580 according to the Figure 8C and D. Moreover, ALP activity, extracellular matrix mineralization and the expression of

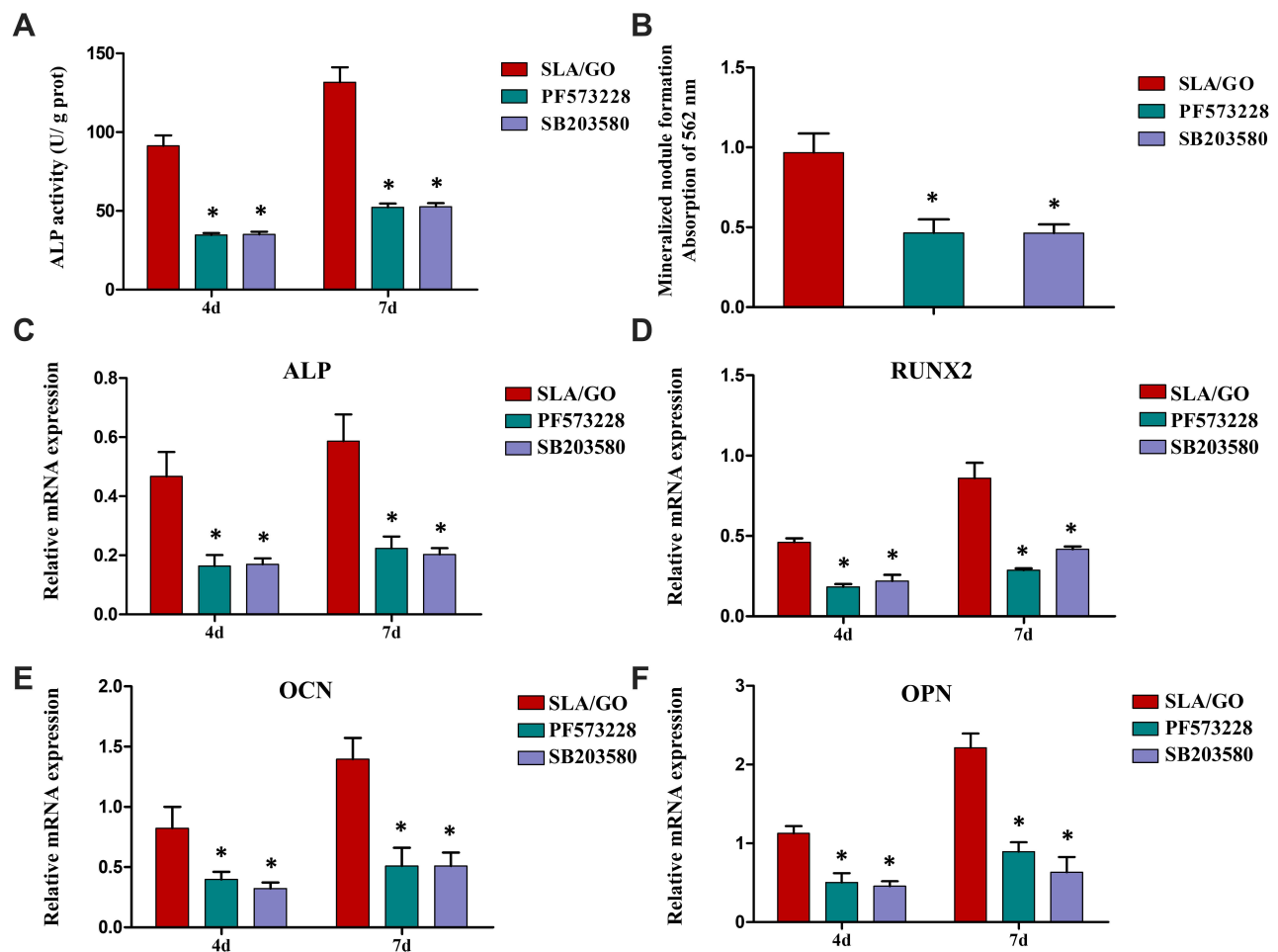


**Figure 9** Osteogenic differentiation of BMSCs cultured on the SLA and SLA/GO samples surface treated with or without specific inhibitors. **(A)** Quantitative analysis of the ALP activity of BMSCs for 4 and 7 days. **(B)** Quantitative analysis of the extracellular matrix mineralization of BMSCs for 21 days. The expressions of osteogenesis-related genes, including ALP **(C)**, RUNX2 **(D)**, OCN **(E)** and OPN **(F)**, were detected by RT-PCR for 4 and 7 days. PF573228 is the inhibitor of FAK and SB203580 is the inhibitor of P38. SLA/GO vs PF573228, SLA/GO vs SB203580, \* $p < 0.05$ .

osteogenesis-related genes (including ALP, RUNX2, OPN, and OCN) in BMSCs cultured on the GO-modified surfaces was also decreased by PF573228 and SB203580 administered separately (Figure 9). These results further confirm that FAK and P38 are involved in the osteogenic differentiation of BMSCs triggered by GO modification.

## Osteogenesis of the GO-Modified Titanium Implants in vivo

### Histological Analysis of BIC

BIC can be used to evaluate the early osseointegration of implants. V-G staining of hard tissue sections revealed that there was new bone tissue formation in the early stage after implantation in both groups of implants (the parts stained red were newly formed bone tissue), but the amount of new bone mass in the GO modification group was higher than that in the control group; in addition, more gaps between bone tissue and

implants were observed around the implants with the SLA surface than around the implants with the GO-modified surface (Figure 10A). The results obtained by ImageJ software analysis showed that the BIC was higher in the GO modification group than in the SLA group at both 2 weeks and 4 weeks after implantation (Figure 10B). This suggests that GO modification can promote early bone-implant osseointegration in vivo.

### Sequential Fluorescence Double Labeling for Analysis of Osteogenesis

The results of dynamic fluorescence analysis of osteogenesis are shown in Figure 11A. The black opaque left area is the implant, and the red and green bands parallel to the implant edge represent the new bone at 2 and 4 weeks after the insert of the implant. The immunofluorescence area was quantitatively analyzed by ImageJ software,

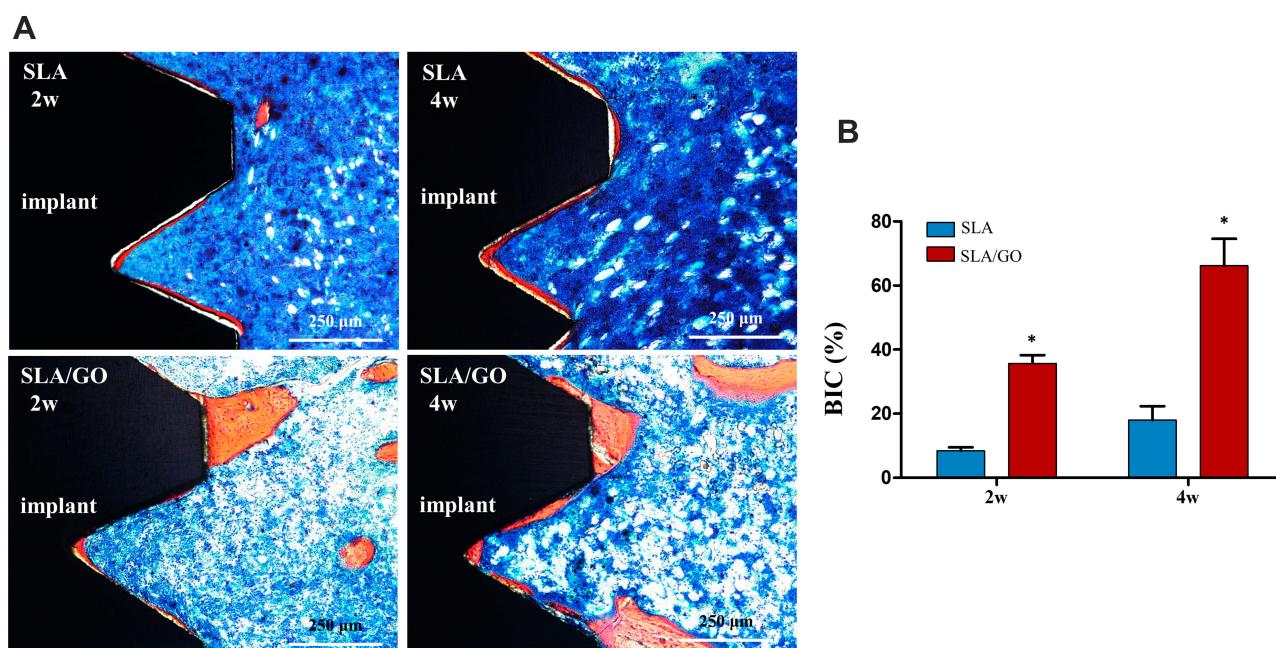


**Figure 10** Osseointegration around the implants with SLA, SLA/GO surfaces in vivo. **(A)** V-G staining of the surrounding tissue of the implants after 2 and 4 weeks and **(B)** analysis of the bone-implant contact (BIC) according to the histological sections images. \* $p < 0.05$ .

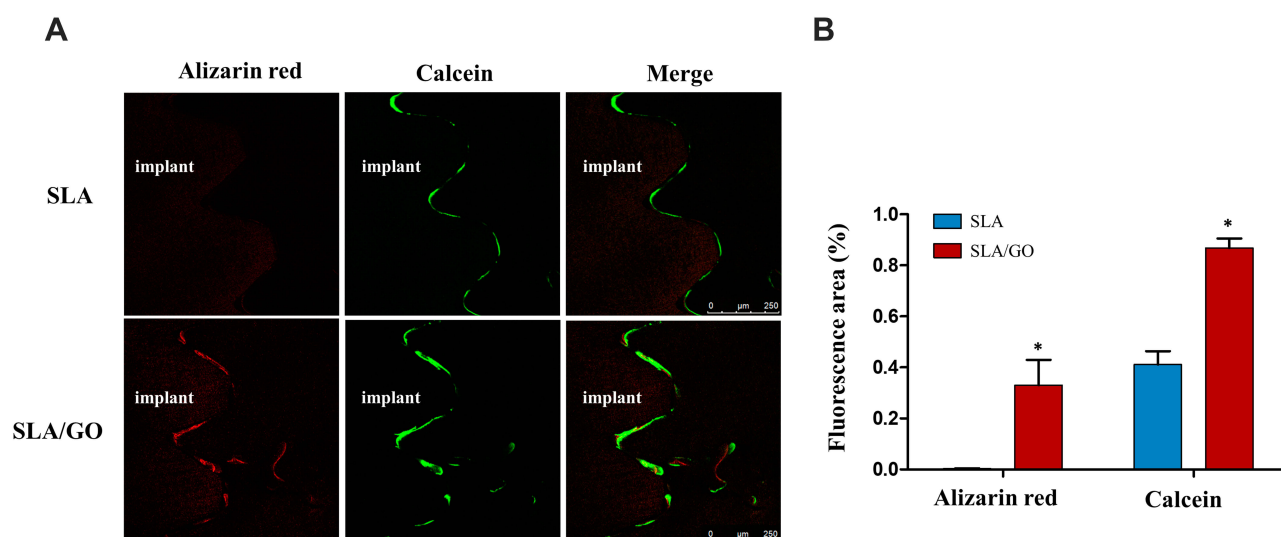


**Figure 11** Osteogenesis around the implants with SLA, SLA/GO surfaces in vivo. **(A)** Sequential fluorescence double labeling of the newly formed bone tissue around the implants after injection of fluorescein (red fluorescence for alizarin red, green for calcein) and **(B)** analysis of the fluorescence area by ImageJ software. \* $p < 0.05$ .

which was shown in Figure 11B. In these two different groups, varying degrees and irregular red and green fluorescent bands were observed around the implants. There was almost no red fluorescence at the SLA implant periphery at 2 weeks, while the SLA/GO group had obvious and clear red bands at 2 weeks and greater fluorescence intensity at 4 weeks. These findings show that the GO coating can promote bone deposition around implants.

Osseointegration is the “golden standard” for evaluation of the success of implants, and the characteristics of an implant surface can regulate the interactions between the material surface and cells, so considerable efforts have been made to optimize surface properties in order to improve the osseointegration of biomaterials. In this study, GO surface modification endowed SLA-treated surfaces with higher hydrophilicity and protein adsorption capacity.

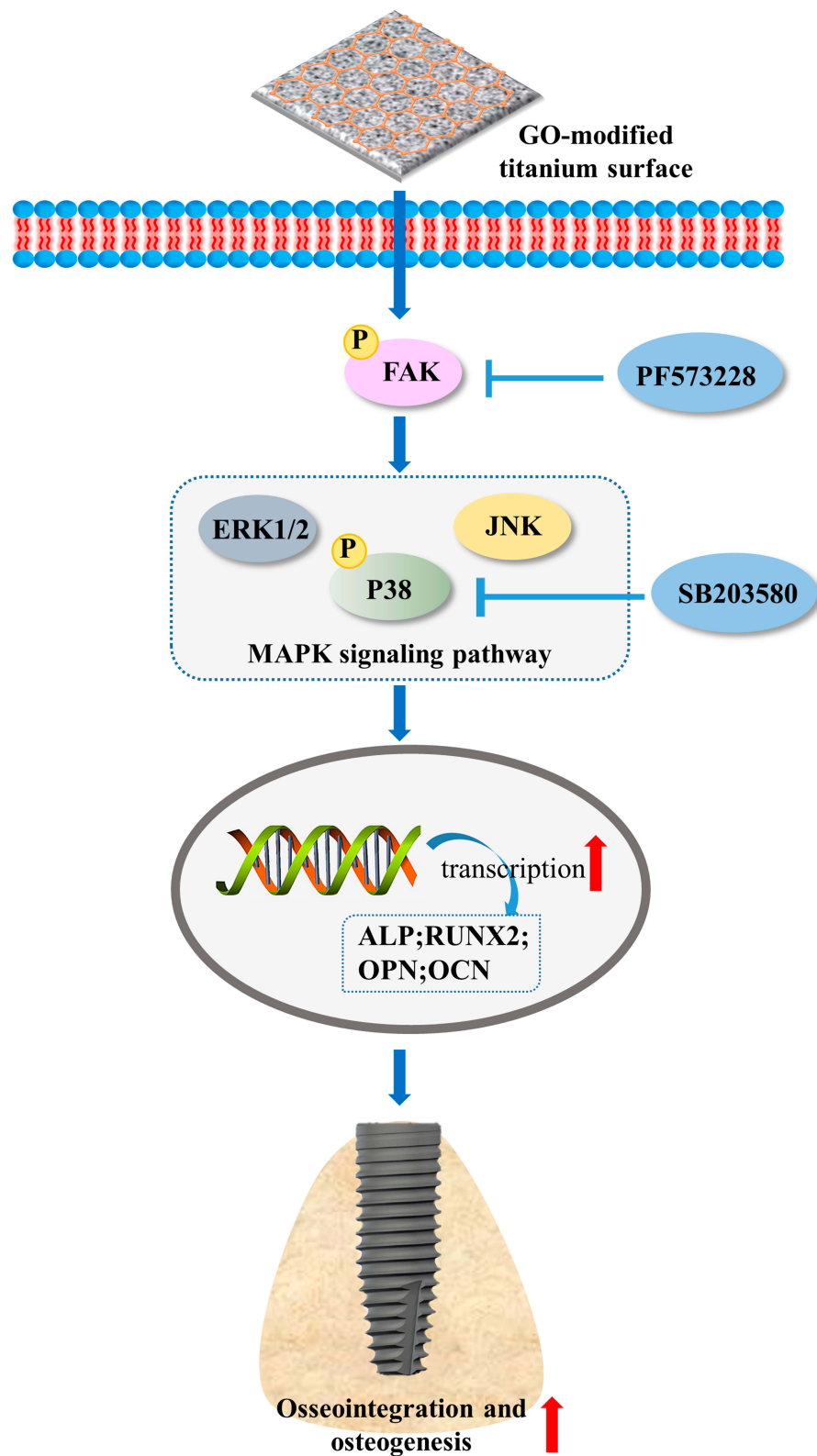


**Figure 12** Schematic illustration of GO modification on SLA-treated titanium surface for osteogenic differentiation of BMSCs and implant osseointegration.

BMSCs proliferation, adhesion and osteogenic differentiation in vitro was also upregulated on GO-modified surface compared with the SLA surface. As key mediator between the intracellular signaling pathways and extracellular stimulation, the expression of focal adhesion was also enhanced on SLA/GO modified surface, which accompanied by the upregulated expression of intracellular focal adhesion kinase (FAK) and its down-streaming MAPK/P38 signaling pathways. In addition, osseointegration efficiency and bone regeneration in vivo was also increased around implants with SLA/GO surface (Figure 12).

## Conclusion

In the present study, the ultrasonic atomization spraying technique was used to develop a GO coating on a titanium surface treated with SLA, which endowed the SLA surface with the enhanced proliferation, adhesion and osteogenic differentiation of BMSCs in vitro. In addition, the FAK/P38 pathways were confirmed to be involved in the improvement of BMSC osteogenic differentiation induced by GO modification. Furthermore, the SLA/GO implants showed excellent osseointegration performance in vivo. Our results provide new evidence that GO modification is a potential implant surface modification method that exerts a positive influence on the bone regeneration. Revealing the mechanism by which materials stimulate osteogenesis and identifying key intracellular events that occur during cell-implant surface interactions may contribute to successful enhancement of osteogenesis, thereby facilitating bone-implant integration.

## Acknowledgments

The authors would like to thank Professor Kaili Lin at the Shanghai Jiao Tong University for assistance with preparing the SLA-treated titanium substrates and Professor Bin Zhao from the University of Shanghai for Science and Technology for helping to prepare the GO coating. In addition, we would like to thank Professor Yao Sun from School of Stomatology of Tongji University for guidance on the writing of this article. This work was financially supported by grants from the National Natural Science Foundation of China (Nos. 81271110 and 81670962), the Fundamental Research Funds for the Central Universities of China (No. 20152957) and the National Key Research and Development Program of China (No. 2018YFE0202200).

## Author Contributions

All authors contributed to data analysis, drafting or revising the article, gave final approval of the version to be published, and agree to be accountable for all aspects of the work.

## Disclosure

The authors report no conflicts of interest in this work.

## References

1. Shibata Y, Tanimoto Y. A review of improved fixation methods for dental implants. Part I: surface optimization for rapid osseointegration. *J Prosthodont Res*. 2015;59(1):20–33. doi:10.1016/j.jpor.2014.11.007
2. Gil FJ, Manzanares N, Badet A, Aparicio C, Ginebra MP. Biomimetic treatment on dental implants for short-term bone regeneration. *Clin Oral Investig*. 2014;18(1):59–66. doi:10.1007/s00784-013-0953-z
3. Liu X, Chu PK, Ding C. Surface modification of titanium, titanium alloys, and related materials for biomedical applications. *Mater Sci Eng R Rep*. 2004;47(3):49–121. doi:10.1016/j.mser.2004.11.001
4. Li Y, Jiao Y, Li X, Guo Z. Improving the osteointegration of Ti6Al4V by zeolite MFI coating. *Biochem Biophys Res Commun*. 2015;460(2):151–156. doi:10.1016/j.bbrc.2015.02.157
5. Gittens RA, Olivares-Navarrete R, Cheng A, et al. The roles of titanium surface micro/nanotopography and wettability on the differential response of human osteoblast lineage cells. *Acta Biomater*. 2013;9(4):6268–6277. doi:10.1016/j.actbio.2012.12.002
6. Civantos A, Martínez-Campos E, Ramos V, Elvira C, Gallardo A, Abarrategi A. Titanium coatings and surface modifications: toward clinically useful bioactive implants. *ACS Biomater Sci Eng*. 2017;3(7):1245–1261. doi:10.1021/acsbmaterials.6b00604
7. Yu Y, Ding T, Xue Y, Sun J. Osteoinduction and long-term osseointegration promoted by combined effects of nitrogen and manganese elements in high nitrogen nickel-free stainless steel. *J Mater Chem B*. 2016;4(4):801–812. doi:10.1039/C5TB02190A
8. Elias CN, Meirelles L. Improving osseointegration of dental implants. *Expert Rev Med Devices*. 2010;7(2):241–256. doi:10.1586/erd.09.74
9. Wennerberg A, Albrektsson T. On implant surfaces: a review of current knowledge and opinions. *Int J Oral Maxillofac Implants*. 2010;25(1):63–74.
10. Le Guehennec L, Soueidan A, Layrolle P, Amouriq Y. Surface treatments of titanium dental implants for rapid osseointegration. *Dent Mater*. 2007;23(7):844–854. doi:10.1016/j.dental.2006.06.025
11. Liu Y, Wang L, Kikui T, et al. Mesenchymal stem cell-based tissue regeneration is governed by recipient T lymphocytes via IFN-gamma and TNF-alpha. *Nat Med*. 2011;17(12):1594–1601. doi:10.1038/nm.2542
12. Yoshizawa S, Brown A, Barchowsky A, Sfeir C. Magnesium ion stimulation of bone marrow stromal cells enhances osteogenic activity, simulating the effect of magnesium alloy degradation. *Acta Biomater*. 2014;10(6):2834–2842. doi:10.1016/j.actbio.2014.02.002
13. Seo HJ, Cho YE, Kim T, Shin HI, Kwun IS. Zinc may increase bone formation through stimulating cell proliferation, alkaline phosphatase activity and collagen synthesis in osteoblastic MC3T3-E1 cells. *Nutr Res Pract*. 2010;4(5):356–361. doi:10.4162/nrp.2010.4.5.356
14. Saidak Z, Marie PJ. Strontium signaling: molecular mechanisms and therapeutic implications in osteoporosis. *Pharmacol Ther*. 2012;136(2):216–226. doi:10.1016/j.pharmthera.2012.07.009
15. Zhang W, Wang G, Liu Y, et al. The synergistic effect of hierarchical micro/nano-topography and bioactive ions for enhanced osseointegration. *Biomaterials*. 2013;34(13):3184–3195. doi:10.1016/j.biomaterials.2013.01.008

16. Tejero R, Anitua E, Orive G. Toward the biomimetic implant surface: biopolymers on titanium-based implants for bone regeneration. *Prog Polym Sci.* **2014**;39(7):1406–1447. doi:10.1016/j.progpolymsci.2014.01.001
17. Miszuk JM, Xu T, Yao Q, et al. Functionalization of PCL-3D electrospun nanofibrous scaffolds for improved BMP2-induced bone formation. *Appl Mater Today.* **2018**;10:194–202. doi:10.1016/j.apmt.2017.12.004
18. Wu SY, An SS, Hulme J. Current applications of graphene oxide in nanomedicine. *Int J Nanomedicine.* **2015**;10(Spec Iss):9–24. doi:10.2147/IJN.S88285
19. Bitounis D, Ali-Boucetta H, Hong BH, Min DH, Kostarelos K. Prospects and challenges of graphene in biomedical applications. *Adv Mater.* **2013**;25(16):2258–2268. doi:10.1002/adma.201203700
20. Gurunathan S, Kim JH. Synthesis, toxicity, biocompatibility, and biomedical applications of graphene and graphene-related materials. *Int J Nanomedicine.* **2016**;11:1927–1945. doi:10.2147/IJN.S105264
21. Shin SR, Li YC, Jang HL, et al. Graphene-based materials for tissue engineering. *Adv Drug Deliv Rev.* **2016**;105(Pt B):255–274. doi:10.1016/j.addr.2016.03.007
22. Kim S, Ku SH, Lim SY, et al. Graphene-biomineral hybrid materials. *Adv Mater.* **2011**;23(12):1237. doi:10.1002/adma.201003669
23. Depan D, Girase B, Shah JS, Misra RD. Structure-process-property relationship of the polar graphene oxide-mediated cellular response and stimulated growth of osteoblasts on hybrid chitosan network structure nanocomposite scaffolds. *Acta Biomater.* **2011**;7(9):3432–3445. doi:10.1016/j.actbio.2011.05.019
24. Tatavarty R, Ding H, Lu G, Taylor RJ, Bi X. Synergistic acceleration in the osteogenesis of human mesenchymal stem cells by graphene oxide-calcium phosphate nanocomposites. *Chem Commun (Camb).* **2014**;50(62):8484–8487. doi:10.1039/C4CC02442G
25. Lee WC, Lim CH, Shi H, et al. Origin of enhanced stem cell growth and differentiation on graphene and graphene oxide. *ACS Nano.* **2011**;5(9):7334–7341. doi:10.1021/nn202190c
26. Liu J, Cui L, Losic D. Graphene and graphene oxide as new nanocarriers for drug delivery applications. *Acta Biomater.* **2013**;9(12):9243–9257. doi:10.1016/j.actbio.2013.08.016
27. Pan Y, Sahoo NG, Li L. The application of graphene oxide in drug delivery. *Expert Opin Drug Deliv.* **2012**;9(11):1365–1376. doi:10.1517/17425247.2012.729575
28. Rana V, Choi MC, Kong JY, et al. Synthesis and drug-delivery behavior of chitosan-functionalized graphene oxide hybrid nanosheets. *Macromol Mater Eng.* **2011**;296(2):131–140. doi:10.1002/mame.201000307
29. Gurunathan S, Han JW, Dayem AA, Eppakayala V, Kim JH. Oxidative stress-mediated antibacterial activity of graphene oxide and reduced graphene oxide in *Pseudomonas aeruginosa*. *Int J Nanomedicine.* **2012**;7:5901–5914. doi:10.2147/IJN.S37397
30. Nanda SS, An SS, Yi DK. Oxidative stress and antibacterial properties of a graphene oxide-cystamine nanohybrid. *Int J Nanomedicine.* **2015**;10:549–556. doi:10.2147/IJN.S75768
31. Mangadlao JD, Santos CM, Felipe MJ, de Leon AC, Rodrigues DF, Advincula RC. On the antibacterial mechanism of graphene oxide (GO) langmuir-blodgett films. *Chem Commun (Camb).* **2015**;51(14):2886–2889. doi:10.1039/C4CC07836E
32. Zhu Y, Cao H, Qiao S, et al. Hierarchical micro/nanostructured titanium with balanced actions to bacterial and mammalian cells for dental implants. *Int J Nanomedicine.* **2015**;10:6659–6674. doi:10.2147/IJN.S92110
33. Jung HS, Lee T, Kwon IK, Kim HS, Hahn SK, Lee CS. Surface modification of multipass caliber-rolled Ti alloy with dexamethasone-loaded graphene for dental applications. *ACS Appl Mater Interfaces.* **2015**;7(18):9598–9607. doi:10.1021/acsami.5b03431
34. La WG, Park S, Yoon HH, et al. Delivery of a therapeutic protein for bone regeneration from a substrate coated with graphene oxide. *Small.* **2013**;9(23):4051–4060. doi:10.1002/sml.201300571
35. Zhang X, Li H, Liu J, et al. Amorphous carbon modification on implant surface: a general strategy to enhance osteogenic differentiation for diverse biomaterials via FAK/ERK1/2 signaling pathways. *J Mater Chem B.* **2019**;7(15):2518–2533. doi:10.1039/C8TB02850H
36. Zhang X, Li H, Lin C, Ning C, Lin K. Synergetic topography and chemistry cues guiding osteogenic differentiation in bone marrow stromal cells through ERK1/2 and p38 MAPK signaling pathway. *Biomater Sci.* **2018**;6(2):418–430. doi:10.1039/C7BM01044C
37. Parsikia F, Amini P, Asgari S. Influence of mechanical and chemical surface treatments on the formation of bone-like structure in cpTi for endosseous dental implants. *Appl Surf Sci.* **2012**;259:283–287. doi:10.1016/j.apsusc.2012.07.033
38. He J, Zhou W, Zhou X, et al. The anatase phase of nanotopography titania plays an important role on osteoblast cell morphology and proliferation. *J Mater Sci Mater Med.* **2008**;19(11):3465–3472. doi:10.1007/s10856-008-3505-3
39. Hung KY, Lo SC, Shih CS, Yang YC, Feng HP, Lin YC. Titanium surface modified by hydroxyapatite coating for dental implants. *Surf Coat Technol.* **2013**;231:337–345. doi:10.1016/j.surfcoat.2012.03.037
40. Cheng M, Qiao Y, Wang Q, et al. Calcium plasma implanted titanium surface with hierarchical microstructure for improving the bone formation. *ACS Appl Mater Interfaces.* **2015**;7(23):13053–13061. doi:10.1021/acsami.5b03209
41. Qiu J, Geng H, Wang D, et al. Layer-number dependent antibacterial and osteogenic behaviors of graphene oxide electrophoretic deposited on titanium. *ACS Appl Mater Interfaces.* **2017**;9(14):12253–12263. doi:10.1021/acsami.7b00314
42. Kudin KN, Ozbas B, Schniepp HC, Prud'homme RK, Aksay IA, Car R. Raman spectra of graphite oxide and functionalized graphene sheets. *Nano Lett.* **2008**;8(1):36–41. doi:10.1021/nl071822y
43. Jeong JT, Choi MK, Sim Y, et al. Effect of graphene oxide ratio on the cell adhesion and growth behavior on a graphene oxide-coated silicon substrate. *Sci Rep.* **2016**;6(1):33835. doi:10.1038/srep33835
44. Zhu Y, Murali S, Cai W, et al. Graphene and graphene oxide: synthesis, properties, and applications. *Adv Mater.* **2010**;22(35):3906–3924. doi:10.1002/adma.201001068
45. Bang SM, Moon HJ, Kwon YD, Yoo JY, Pae A, Kwon IK. Osteoblastic and osteoclastic differentiation on SLA and hydrophilic modified SLA titanium surfaces. *Clin Oral Implants Res.* **2014**;25(7):831–837. doi:10.1111/clr.12146
46. Jia Z, Shi Y, Xiong P, et al. From solution to biointerface: graphene self-assemblies of varying lateral sizes and surface properties for biofilm control and osteodifferentiation. *ACS Appl Mater Interfaces.* **2016**;8(27):17151–17165. doi:10.1021/acsami.6b05198
47. Park J, Kim B, Han J, et al. Graphene oxide flakes as a cellular adhesive: prevention of reactive oxygen species mediated death of implanted cells for cardiac repair. *ACS Nano.* **2015**;9(5):4987–4999. doi:10.1021/nn507149w
48. Yang K, Gong H, Shi X, Wan J, Zhang Y, Liu Z. In vivo biodistribution and toxicology of functionalized nano-graphene oxide in mice after oral and intraperitoneal administration. *Biomaterials.* **2013**;34(11):2787–2795. doi:10.1016/j.biomaterials.2013.01.001
49. Kanakia S, Toussaint JD, Chowdhury SM, et al. Dose ranging, expanded acute toxicity and safety pharmacology studies for intravenously administered functionalized graphene nanoparticle formulations. *Biomaterials.* **2014**;35(25):7022–7031. doi:10.1016/j.biomaterials.2014.04.066
50. Mao L, Liu J, Zhao J, et al. Effect of micro-nano-hybrid structured hydroxyapatite bioceramics on osteogenic and cementogenic differentiation of human periodontal ligament stem cell via Wnt signaling pathway. *Int J Nanomedicine.* **2015**;10:7031–7044. doi:10.2147/IJN.S90343
51. Lin K, Xia L, Gan J, et al. Tailoring the nanostructured surfaces of hydroxyapatite bioceramics to promote protein adsorption, osteoblast growth, and osteogenic differentiation. *ACS Appl Mater Interfaces.* **2013**;5(16):8008–8017. doi:10.1021/am402089w

52. Petit V, Thiery JP. Focal adhesions: structure and dynamics. *Biol Cell*. 2000;92(7):477–494. doi:10.1016/S0248-4900(00)01101-1
53. Critchley DR. Focal adhesions - the cytoskeletal connection. *Curr Opin Cell Biol*. 2000;12(1):133–139. doi:10.1016/S0955-0674(99)00067-8
54. Wang H, Lin C, Zhang X, Lin K, Wang X, Shen SG. Mussel-inspired polydopamine coating: a general strategy to enhance osteogenic differentiation and osseointegration for diverse implants. *ACS Appl Mater Interfaces*. 2019;11(7):7615–7625. doi:10.1021/acsami.8b21558
55. Salasnyk RM, Klees RF, Williams WA, Boskey A, Plopper GE. Focal adhesion kinase signaling pathways regulate the osteogenic differentiation of human mesenchymal stem cells. *Exp Cell Res*. 2007;313(1):22–37. doi:10.1016/j.yexcr.2006.09.013
56. Mitra SK, Hanson DA, Schlaepfer DD. Focal adhesion kinase: in command and control of cell motility. *Nat Rev Mol Cell Biol*. 2005;6(1):56–68. doi:10.1038/nrm1549
57. So EC, Wu KC, Liang CH, Chen JY, Wu SN. Evidence for activation of BK Ca channels by a known inhibitor of focal adhesion kinase, PF573228. *Life Sci*. 2011;89(19–20):691–701. doi:10.1016/j.lfs.2011.08.013
58. Slack-Davis JK, Martin KH, Tilghman RW, et al. Cellular characterization of a novel focal adhesion kinase inhibitor. *J Biol Chem*. 2007;282(20):14845–14852. doi:10.1074/jbc.M606695200
59. English JM, Cobb MH. Pharmacological inhibitors of MAPK pathways. *Trends Pharmacol Sci*. 2002;23(1):40–45. doi:10.1016/S0165-6147(00)01865-4

## International Journal of Nanomedicine

Dovepress

### Publish your work in this journal

The International Journal of Nanomedicine is an international, peer-reviewed journal focusing on the application of nanotechnology in diagnostics, therapeutics, and drug delivery systems throughout the biomedical field. This journal is indexed on PubMed Central, MedLine, CAS, SciSearch®, Current Contents®/Clinical Medicine,

Journal Citation Reports/Science Edition, EMBASE, Scopus and the Elsevier Bibliographic databases. The manuscript management system is completely online and includes a very quick and fair peer-review system, which is all easy to use. Visit <http://www.dovepress.com/testimonials.php> to read real quotes from published authors.

Submit your manuscript here: <https://www.dovepress.com/international-journal-of-nanomedicine-journal>